European Journal of Medicinal Chemistry 156 (2018) 790–799

Contents lists available at ScienceDirect

European Journal of Medicinal Chemistry

journal homepage: http://www.elsevier.com/locate/ejmech

Research paper

Structure-activity relationships of anticancer ruthenium(II) complexes with substituted hydroxyquinolines

Dmytro Havrylyuk, Brock S. Howerton, Leona Nease, Sean Parkin, David K. Heidary**, Edith C. Glazer*

Department of Chemistry, University of Kentucky, 505 Rose Street, Lexington, KY 40506, United States

ARTICLE INFO

Article history:
Received 21 February 2018
Received in revised form
16 April 2018
Accepted 21 April 2018
Available online 30 April 2018

Keywords:
Cytotoxic
Ruthenium
Cancer
Coordination chemistry
Translation

ABSTRACT

8-Hydroxyquinolines (HQ), including clioquinol, possess cytotoxic properties and are widely used as ligands for metal-based anticancer drug research. The number and identity of substituents on the HQ can have a profound effect on activity for a variety of inorganic compounds. Ruthenium complexes of HQ exhibit radically improved potencies, and operate by a new, currently unknown, mechanism of action. To define structure-activity relationships (SAR), a family of 22 Ru(II) coordination complexes containing mono-, di- and tri-substituted hydroxyquinoline ligands were synthesized and their biological activity evaluated. The complexes exhibited promising cytotoxic activity against a cancer cell line, and the SAR data revealed the 2- and 7-positions as key sites for the incorporation of halogens to improve potency. The Ru(II) complexes potently inhibited translation, as demonstrated by an in-cell translation assay. The effects were seen at 2–15-fold higher concentrations than those required to observe cytotoxicity, suggesting that prevention of protein synthesis may be a primary, but not the exclusive mechanism for the observed cytotoxic activity.

1. Introduction

Coordination complexes containing 8-hydroxyquinoline ligands (HQ) have shown promise for the development of small molecule drugs, particularly in anticancer research [1]. Most notably, tris-8-HQ gallium(III) (KP46) has reached clinical evaluation in phase I trials, and exhibited activity in the treatment of renal cell carcinoma [2]. This complex was discovered and patented due to its potential efficacy for treating pancreatic cancer [3], and was also highly active against osteosarcoma cells by inducing cancer cell death via a p53 dependent mechanism, and inhibiting cellular migratory potential [4].

Various other metal complexes of HQ ligands have been investigated, with a range of oxidation states and coordination numbers. These include silver (I) [5], copper(II) [6], platinum(II) [7], cobalt(II) [8], zinc(II) [9], gold(III) [10], and rhodium(III) [11]. Both unsubstituted and substituted HQ ligands have been incorporated into complexes, but often the individual studies described only a few systems, preventing any conclusive structure-activity relationship (SAR) conclusions from being drawn. In other cases, conflicting SAR patterns have been reported. For example, a Pt(II) complex with unsubstituted HQ was identified as the most active in specific cell lines, while a Pt(II) complex with clioquinol possessed the highest cytotoxicity in others [7b], and the complex bearing the 5,7-diiodo-HQ ligand was the more potent entity in a different study [7c]. In nearly all cases of homoleptic metal complexes, though, the free HQ ligands were less potent than corresponding coordination complexes. For example, cobalt(II) complex of 5-chloro-8-hydroxyquinoline showed higher cytotoxicity than the corresponding metal salt ($Co(NO_3)_2 \cdot 6H_2O$) and the free ligand when tested with five tumor cell lines [8a]. Complexes of 5,7-dihalo-HQs with lanthanides [12], tin(IV) [13], nickel(II) [14], zinc(II), copper(II) [15], cerium(III, IV) [16] and iron(III) [17] have been reported, and the complexes exhibited significantly enhanced cytotoxicities compared to parent HQ ligands, with single micromolar to nanomolar IC_{50} values.

Less common are metal complexes containing only one HQ ligand, and in these cases metal coordination can increase or decrease potency, depending on the other components of the system. A study performed by Hartinger and coworkers investigated coordination of HQs ligands to a Ru(II) (η^6-*p*-cymene) scaffold,

* Corresponding author.
** Corresponding author.
E-mail address: ec.glazer@uky.edu (E.C. Glazer).

https://doi.org/10.1016/j.ejmech.2018.04.044
0223-5234/

where halogens at the 5- and 7-positions of the HQ ligand were systematically varied [18]. In this report the metal complexes were less potent than the corresponding free ligands, and little variation was found with regards to the identity of the halogen. In other reports, coordination resulted in decreases or only modest improvements in potency [19]. In contrast, we previously demonstrated that the coordination of HQs to the [Ru(dmphen)$_2$] scaffold (dmphen = 2,9-dimethyl-1,10-phenanthroline) yielded a significant improvement in cytotoxicity compared to the parent ligands, with potencies up to 86-fold greater than clioquinol [1a]. The complexes were also >100-fold more potent than clioquinol in a 3D tumor spheroid model, with values similar to chemotherapeutics currently used for the treatment of solid tumors. We observed that the Ru(II) scaffold played a major role in driving the potency of the complexes, with compounds containing bpy coligands being far less active. Two similar molecules were investigated *in vivo* by Liu and coworkers, with the 8-hydroxyquinoline ligand coordinated to Ru(II) centers containing either 2,2′-bipyridine (bpy) or 1,10-phenanthroline (phen) coligands. They showed promising inhibition of angiogenesis and tumor growth, with effects observed for the phen complex at concentrations of 8 mg kg^{-1}d^{-1} [20]. Thus, Ru(II) heteroleptic complexes containing HQ ligands possess noteworthy activity both *in vitro* and *in vivo*.

These findings have motivated us to pursue a comprehensive SAR investigation of Ru(II) complexes with mono-, di- and tri-substituted hydroxyquinoline ligands in order to identify the optimal structural frameworks for further medicinal chemistry efforts. The main goal of this study was to answer the following questions: 1) Does the nature of the substituent (halogens vs. methyl or aryl groups) influence the cytotoxic effect? 2) What positions of HQ should be modified for enhanced activity?

2. Results and discussion

2.1. Chemistry

Our earlier SAR analysis of HQ complexes with the [Ru(dmphen)$_2$] scaffold revealed that the presence of halogens at the 5- and 7-positions resulted in the most potent compounds, while incorporation of electron rich substituents such as a nitro group or sulfonic acids at the 5-position of the hydroxyquinoline reduced potency up to 220-fold [1a]. Therefore, in this study we focused on halogen-, methyl- and aryl-substituted HQs, generating complexes with mono-, di- and tri-substituted HQ ligands. The Ru(II) complexes were synthesized from a racemic mixture of the Δ and Λ enantiomers of [Ru(dmphen)$_2$Cl$_2$] and form a mixture of enantiomers upon coordination of the hydroxyquinoline ligand [1a]. All complexes were exhaustively purified to ensure no contamination of either free ligands or coordinatively unsaturated Ru(II) center. The yields were moderate or low for some complexes, due in part to the fact that the [Ru(dmphen)$_2$] scaffold is sterically congested.

Aiming to identify the impact of halogen substitution on the biological activity, the analogous chloro- and bromo-substituted HQ ligands were used. To allow for comparison of variation is the radius of the substituent, as well as its electronic nature, a methyl-substituted HQ was also investigated. In order to introduce a larger substituent, the Ru(II) complexes with 5- (compound **6**) or 7-bromo-HQs (compound **9**) were modified via the Suzuki coupling reaction, yielding ruthenium compounds **8** and **11** with aryl-substituted HQ ligands. Interestingly, the synthesis of the analogous 2-substituted compound, **5**, failed on the metal complex. This was hypothesized to be due to steric constraints, despite successful Ru(II) center to form compound **5**. Both complexes **5** and **11** displayed a single resonance for the Me group in ^{1}H NMR spectra, but resonances for Me groups of the *o*-tolyl fragment of complex **8** were resolved as two singlets. This indicated restricted rotation of the o-tolyl fragment and presence of two rotamers with 2:3 ratio.

Under the reaction conditions for the coordination of 7-chloro-HQ to the [Ru(dmphen)$_2$] scaffold in ethanol-water medium (1:1), the complex unexpectedly underwent an oxidative coupling (dimerization), producing the Ru(II) dimer **22** linked at the 5 position of the HQ rings (Scheme S1). The structure of **22** was confirmed by ^{1}H NMR and ESI MS spectra (Figs. S28 and 29) and X-ray, as discussed below.

2.2. Crystallography

The structures of complexes **2**, **9** and **14** were determined by X-ray crystallography (Fig. 1, Fig. S1-3). Selected bond lengths and angles are listed in Table 1.

All complexes exhibited distorted octahedral geometries. The incorporation of two dmphen ligands and HQ resulted in shortening of the Ru–N(dmphen) bonds to 2.093 Å (average value for **2**), 2.096 Å (average value for **9**), and 2.089 Å (average value for **14**) in comparison with analogous complex containing 2,3-dihydro-1,4-dioxino [2,3-f]-1,10-phenanthroline [21] or pyridyl-benzazole [22] on the [Ru(dmphen)$_2$] scaffold, where the average values are 2.103–2.117 Å. Introduction of a methyl group into position 2 of the HQ (**2**) caused the Ru-N5 bond to lengthen to 2.162 Å in comparison to complexes **9** and **14**. The Ru-O bonds are longer for compounds **9** and **14**, most likely due to the presence of halogens at the 7-position of HQs. The bond angles between the dmphen and HQ ligands are nonequivalent, with the largest distortion of L1 (dmphen where L is N1 and N2) for complex **14** (Fig. 1C). The angles change from the ideal 90° to 79.05–105.38° and 180° to 168.58–177.02°. Both the dmphen ligands (L1 and L2, Fig. 1, Table 1) for each compound are considerably bent from the normal plane,

Table 1
Selected bond lengths [A], bond angles [°] and torsion angles [°] of **2**, **9** and **14**.

	2	9	14
Bond Lengths (Å)			
Ru-N1	2.111(2)	2.114(2)	2.1048(16)
Ru-N2	2.0852(19)	2.095(2)	2.0859(16)
Ru-N3	2.081(2)	2.079(2)	2.0757(16)
Ru-N4	2.097(2)	2.099(2)	2.0891(16)
Ru-N5	2.162(2)	2.063(2)	2.0718(16)
Ru-O	2.0537(16)	2.0924(19)	2.0789(13)
Bond Angles (°)			
N1-Ru-N2	80.12(8)	80.03(9)	79.53(6)
N1-Ru-N3	103.64(8)	103.16(9)	105.38(6)
N1-Ru-N4	176.24(7)	176.40(9)	174.49(6)
N1-Ru-N5	97.20(7)	98.10(9)	95.65(6)
N1-Ru-O	79.29(7)	79.86(8)	79.05(6)
N2-Ru-N3	94.36(7)	93.74(9)	97.39(6)
N2-Ru-N4	98.32(8)	100.58(9)	99.46(6)
N2-Ru-N5	166.58(8)	171.70(9)	168.58(6)
N2-Ru-O	86.68(7)	91.96(8)	88.79(6)
N3-Ru-N4	79.85(8)	80.36(9)	80.11(7)
N3-Ru-N5	99.05(8)	94.56(9)	93.87(6)
N3-Ru-O	177.02(7)	173.93(8)	172.92(6)
N4-Ru-N5	83.52(7)	80.79(9)	84.34(6)
N4-Ru-O	97.24(7)	96.56(8)	95.53(6)
N5-Ru-O	79.90(7)	79.74(8)	80.09(6)
L1 bend[a]	19.7	14.2	23.1
L2 bend[b]	8.3	11.4	9.6

[a] L1 bend = 90° − average angle (O-Ru-C13/C14); L1 - dmphen where L is N1 and

reaction at the 7-poistion, which is also partially occluded by the coordinated Ru(II) center. As a result, the free ligand was first subjected to the coupling reaction and then coordinated to the

N2, as example for complex **2**.

[b] L2 bend = 90° − average angle (N5-Ru-C27/C28); L2 - dmphen where L is N3 and N4, as example for complex **2**.

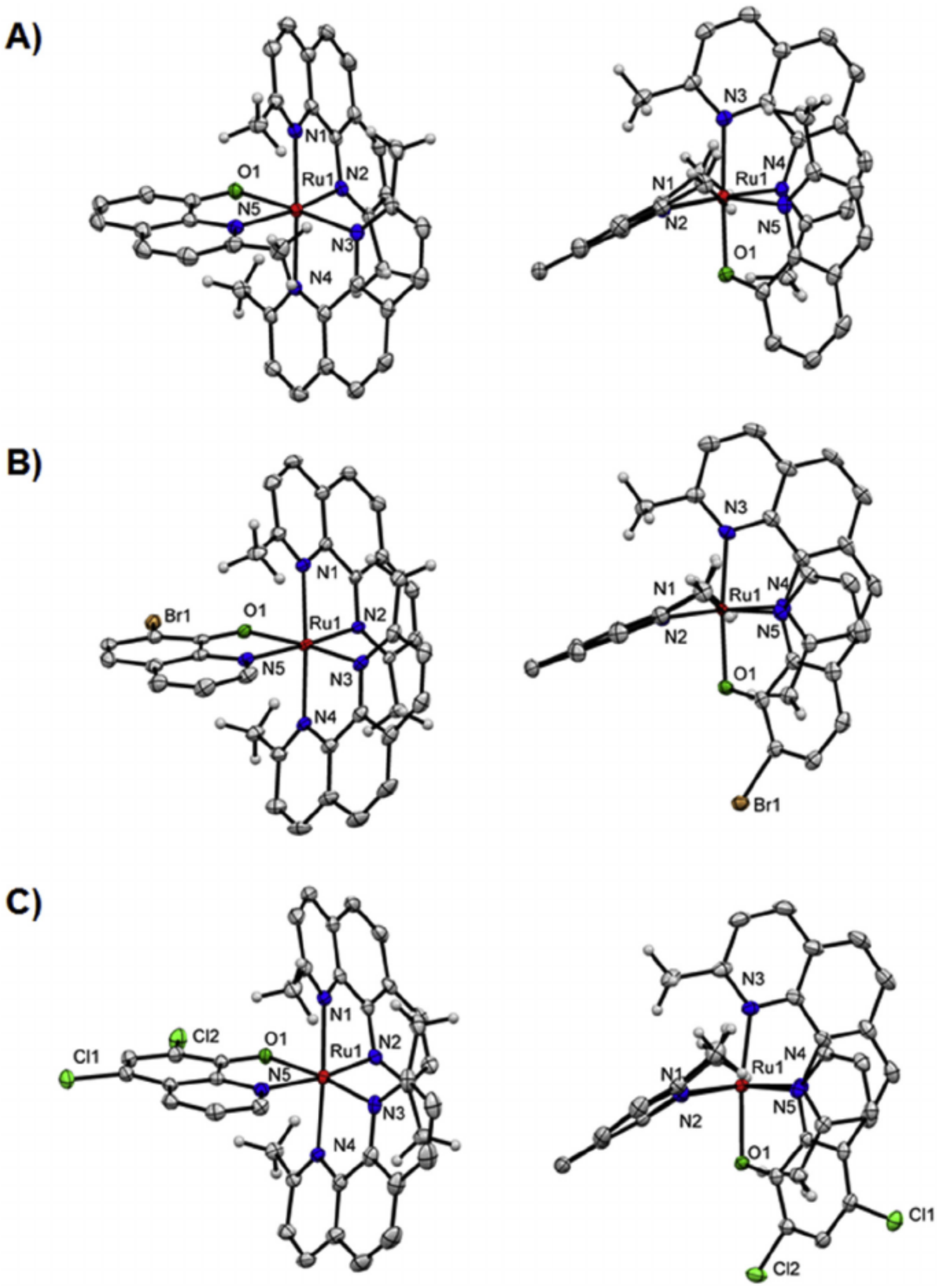

Fig. 1. Ellipsoid plot of ruthenium complexes: (A) (*Δ*)-**2**, (B) (*Δ*)-**9**, (C) (*Δ*)-**14** at 50% probability with H atoms omitted for clarity. Right column: side views, highlighting the distortion of the dmphen ligand.

with deviations of 8.3–23.1°. While the bend angles for both dmphen ligands in complex **9** are similar, the bends of L1 for compounds **2** and **14** are significantly larger than those for L2.

For the dimer **22**, the crystals were twinned by non-merohedry and diffracted poorly, giving diffuse but indexable, Bragg diffraction to not quite 1 Å resolution. Although the structure solved with relative ease, it did not refine to commonly accepted standards. Nevertheless, the connectivity of the molecule is consistent with the dimerization between the HQ rings at the 5-position. A cartoon of the structure, inspired by the x-ray data, is shown in Fig. S30.

HQs, six that were di-substituted, and four tri-substituted analogs, and compared them to the corresponding complex with the unsubstituted HQ ligand (Table 2, Figs. 2 and 3). The data for four complexes (**1**, **2**, **14** and **16**) have been previously published [1a].

The initial SAR study for the ruthenium complexes coordinated with HQ was based on the incorporation of a single substituent (a halogen or Me group) into hydroxyquinoline. The comparison of complexes with 2-substituted HQ ligands showed that the potency depends on the nature of substituent. The presence of a halogen at the 2-position of HQ improved the cytotoxicity of complexes by

2.3. Cytotoxicity studies

To generate SAR to understand and rationally modulate the biological activity of the Ru(II) complexes, we studied the cytotoxicity in HL60 cells of ten compounds with mono-substituted

Table 2
Cytotoxicity IC_{50} values (μM) for Ru(II) complexes in the HL60 cancer cell line.

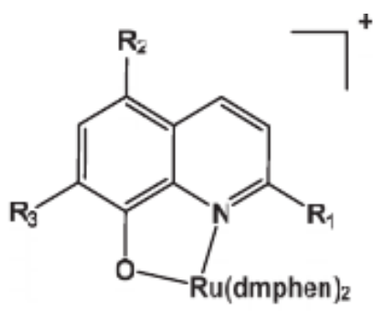

Compound	R_1	R_2	R_3	IC_{50}, (μM)
mono-substituted HQs				
1	H	H	H	0.52 ± 0.06 [a]
2	Me	H	H	0.49 ± 0.07 [a]
3	Br	H	H	0.18 ± 0.015
4	Cl	H	H	0.11 ± 0.003
5	o-tolyl	H	H	0.20 ± 0.069
6	H	Br	H	0.32 ± 0.013
7	H	Cl	H	0.43 ± 0.04
8	H	o-tolyl	H	0.67 ± 0.19
9	H	H	Br	0.10 ± 0.018
10	H	H	Cl	0.09 ± 0.004
11	H	H	o-tolyl	0.96 ± 0.11
di-substituted HQs				
12	H	Me	Me	0.18 ± 0.015
13	H	Br	Br	0.07 ± 0.008
14	H	Cl	Cl	0.11 ± 0.006 [a]
15	H	Cl	Br	0.09 ± 0.034
16	H	Cl	I	0.057 ± 0.002
17	H	I	I	0.12 ± 0.004
tri-substituted HQs				
18	Me	Me	Me	0.25 ± 0.051
19	Me	Br	Br	0.08 ± 0.02
20	Me	Cl	Cl	0.12 ± 0.002
21	Cl	Br	Br	0.07 ± 0.009
Ru(II) dimer				
22	H	–	Cl	11.14 ± 0.658

[a] Previously reported data [1a].

complexes that were 2–4 fold less potent by than analogous compounds with halogens at the 2-position (**3** and **4**), though the compounds were more potent than compound **1**. The highest activities were identified for complexes with 7-bromo-and 7-chloro-HQs (**9** and **10**). Incorporation of the halogen at the 7-position resulted in at least 5-fold increases of activity compared to complex **1**, with IC_{50} values ≈ 100 nM.

Arylation of the 5- and 7-positions reduced the potencies of the compounds. The IC_{50} value for the complex containing 7-(o-tolyl)-HQ (**11**) shifted to 0.96 μM, which is approximately 2-fold less potent than the parent complex **1** and 10-fold less potent than the value observed for the 7-bromo complex **9**. The IC_{50} value was 0.67 μM for the complex containing 5-(o-tolyl)-HQ (**8**), 2-fold less potent than the value observed for the 5-bromo complex **6**. Interestingly, the opposite trend was observed for arylation at the 2-position, with complex **5** being approximately 2-fold more potent than the parent complex **1** and having the same IC_{50} value as the 2-bromo complex **3**. Thus, significant variation in potencies were found, with values spanned the range from 0.09 to 0.96 μM. The trends for potencies of monosubstituted HQs coordinated with Ru(II) scaffold and were as follows: 7-(o-tolyl)-HQ (**11**) < 5-(o-tolyl)-HQ (**8**) < HQ (**1**) ≈ 2-Me-HQ (**2**) < 5-Cl-HQ (**7**) < 5-Br-HQ (**6**) < 2-(o-tolyl)-HQ (**5**) ≈ 2-Br-HQ (**3**) < 2-Cl-HQ (**4**) ≈ 7-Br-HQ (**9**) ≈ 7-Cl-HQ (**10**).

Further SAR analysis was focused on the incorporation of two or three substituents into the HQ ligand. In contrast to mono-methyl substituted system (complex **2**), the addition of methyl groups at 5- and 7-positions (complex **12**) improved the potency by 3-fold compared to **1**, but the dimethyl complex was less active compared to dihalogenated compounds (**13**–**17**). Despite the absence of a radical improvement in cytotoxicity of 5,7-dihalogen substituted HQs (**13**–**17**) in comparison with 7-bromo- or 7-chloro-analogs (**9** and **10**), it should be noted that three of the five compounds possessed activity against the HL60 cell line with IC_{50} values lower than 100 nM. Complex **13**, with 5,7-dibromo-HQ (IC_{50} = 70 nM), and **15**, with 5-chloro-7-bromo-HQ (IC_{50} = 87 nM), possessed the same range of activity as complex containing clioquinol (**16**, IC_{50} = 57 nM; Fig. 2B). As clioquinol and its complexes undergo degradation due to a deiodination reaction [23], complexes **13** and **15** are preferable lead compounds for further medicinal chemistry efforts as both were found to be stable as well as potent.

Interestingly, halogen size does not appear to be the primary driver for activity, as both the dichloro-HQ (**14**) and diiodo-HQ (**17**) were slightly less potent than the dibromo-HQ **13** and **15**, with IC_{50} values of 110–120 nM. The addition of a third substituent (Me or Cl) at the 2-position resulted in the same IC_{50} values as analogous disubstituted systems, except for complex **20**. Thus, compounds **19** and **21** possessed the same range of activity as complex **13**, with IC_{50} values of 68–77 nM. Finally, while the monomethyl HQ complex was no better than an unsubstituted HQ, the trimethyl HQ complex **18** was twice as potent, but the presence of the third methyl group at the 2-position was somewhat deleterious (250 nM for **18** vs. 180 nM for compound **12**).

Notably, the Ru(II) dimer (compound **22**) possessed the lowest potency, with IC_{50} value of 10.01 μM. This dimer was less potent than the previously reported analogous monomer containing a nitro group at the 5-position (IC_{50} = 2.31 μM). Only the complex

Fig. 2. Cytotoxicity dose responses of ruthenium complexes on HL60 cells: (A) activity of Ru(II) complexes with mono-substituted HQ ligands containing bromine at 2- (**3**), 5- (**6**) and 7-positions (**9**), compared to complex containing 7-(o-tolyl)-HQ (**11**); (B) activity of Ru(II) complexes with di-substituted HQ (**13**) and tri-substituted HQ (**19**), compared to the complex containing clioquinol (**16**).

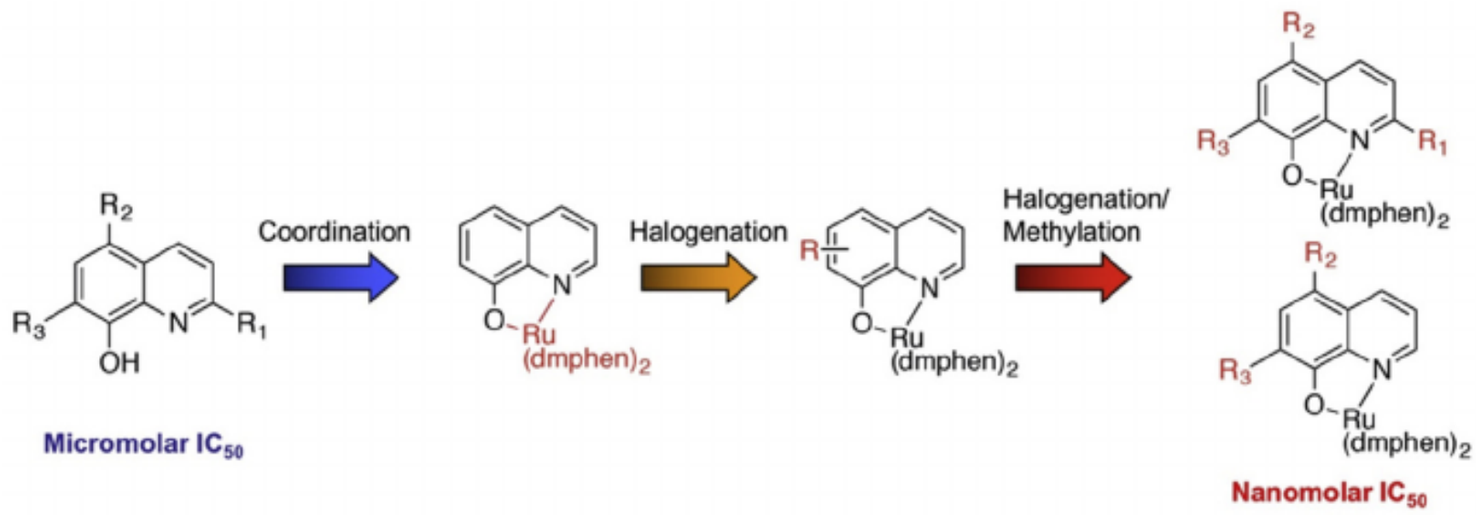

Fig. 3. Structure-activity relationships for cytotoxicity based on analysis of Ru(II) complexes with mono-, di-, and tri-substituted HQ ligands. Potency increases upon coordination, and further increases with addition of a single halogen, followed by two or three halogen or methyl substituents. Systems containing two or three substituents show equal potencies.

containing a sulfonic acid at the same position was less potent, with no toxicity observed at concentrations up to 30 μM [1a]. Thus, it appears that the 5-position is sensitive to both steric bulk and electron rich substituents; potent compounds can only be achieved with smaller substituents such as halogens, methyl groups, or a single aromatic ring.

The main findings of the SAR analysis (Fig. 3) illustrated that: 1) incorporation of a halogen at positions 2 and 7 is crucial for improvement of potency, but the nature of the halogen does not result in radical shifts; 2) the presence of an additional halogen at position 5 slightly improved potencies in comparison to 7-monosubstituted analogs, and resulted in IC_{50} values lower than 100 nM; 3) arylation of the 5- or 7-position significantly reduced the activity, while arylation at the 2-position *increased* activity; 4) a Ru(II) dimer linked at the 5-position of the HQ ligand possessed the lowest potency among described compounds.

2.4. In-cell transcription and translation assay

The cytotoxic mechanism of action for hydroxyquinoline ligands has been previously reported to occur through inhibition of the proteasome [24]. Recently, it was demonstrated that clioquinol induced pro-death autophagy in leukemia and myeloma cells by disrupting the mTOR signaling pathway [25]. The mechanistic effects of various metal complexes containing HQ ligands are diverse, and we previously demonstrated that the ruthenium complex with clioquinol did not inhibit the proteasome at concentrations relevant for cell death [1a]. In order to investigate the effect of the HQ complexes on essential biological processes, a cell-based transcription and translation assay was performed using Dendra2 as a reporter for protein synthesis. This allowed for a real-time report in live cells of any damage to the DNA, RNA, or the ribosome, or inhibition of any essential components of the cellular machinery responsible for the processes of transcription and translation [26]. Dendra2 is a photoconvertable protein; upon irradiation, Dendra2 switches from green to red fluorescence, while Dendra2 synthesized after irradiation will only show green fluorescence. Therefore, this assay allows for the real-time observation of newly-synthesized protein with ratiometric detection compared to previously made protein, providing an assay for inhibition of protein synthesis that can be assessed in dose response and with kinetic information.

Five potent complexes (**4**, **13**, **15**, **19** and **20**) and two associated ligands (2-methyl-5,7-dibromo-HQ and 2-methyl-5,7-dichloro-HQ) were tested for potential effects on protein synthesis. Rapamycin was used as a positive control, with the results shown in Fig. 4A. Inhibition of protein synthesis was observed for rapamycin with an IC_{50} of 6.3 μM. The free ligand 2-methyl-5,7-dichloro-HQ was more potent, with an IC_{50} of 1.6 μM. Notably, this value corresponds closely to the cytotoxicity of compound in the HL60 cell line ($IC_{50} = 0.55$ μM, Fig. S5). The 2-methyl-5,7-dibromo-HQ was slightly less potent at 3.34 μM (Fig. S4). Complex **20**, [Ru(dmphen)$_2$-2-Me-5,7-diCl-HQ], had the same effect, but it occurred at lower doses and with a steeper dose response, where 0.54 μM was required for 50% inhibition of translation and 1 μM led to an 80% reduction in Dendra2 production (Fig. 4A and Fig. S6). The most potent inhibition in the Dendra2 assay was observed for compound **4** ($IC_{50} = 0.29$ μM), while compounds **13** ($IC_{50} = 1.0$ μM), **15** ($IC_{50} = 0.46$ μM), and **19** ($IC_{50} = 0.92$ μM) were 1.5–3-times less potent (Fig. 4B). No degradation was seen for the photoconverted Dendra2 over the course of the assay, indicating the compounds did not affect degradation of existing proteins.

In general, the tested complexes exhibited effective inhibition of Dendra2 at IC_{50} values < 1 μM; however, these concentrations are 2–14 times higher than required for cytotoxicity. These data suggest that inhibition of translation is likely involved but may not be

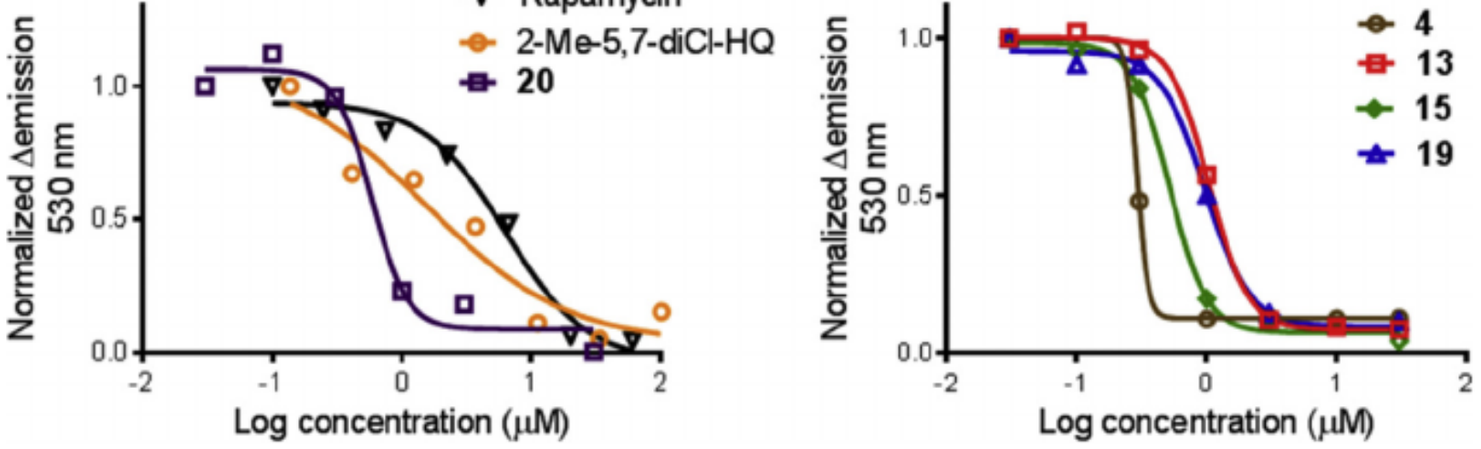

Fig. 4. Inhibition of protein synthesis dose responses of ruthenium complexes in Dendra2 assay: (A) activity of Ru(II) complex **20**, compared with parent ligand (2-methyl-5,7-dichloro-8-hydroxyquinoline) and rapamycin; (B) activity of Ru(II) complexes **4**, **13**, **15** and **19**.

the exclusive mechanism that induces the cytotoxicity of Ru(II) HQ complexes.

3. Conclusions

Quinoline and hydroxylquinoline are considered privileged structures, as these heterocycles are found in a wide range of naturally occurring and synthetic biologically active molecules that interact with diverse targets, inducing functional changes of importance in a variety of disease states. These features suggest a variety of possible mechanisms of action and biological interaction partners, leading to complex and inconsistent structure-activity relationships, depending on both the functional assay and biological test system chosen. Further complicating the situation, many hydroxyquinolines under investigation coordinate various metals, acting as ionophores to increase cellular uptake, but they can also transport the metals to difference subcellular compartments or form semi-stable metal complexes that could participate in redox reactions. Alternatively, the transient metal complexes could directly bind and regulate the activity of important biomolecules. Stable metal complexes, in contrast, present a simpler case, as metal transport properties are eliminated, and in most cases, redox cycling or covalent adduct formation is not possible. This leaves direct, but non-covalent, interactions with biological targets as the most likely source for the observed activity.

This detailed SAR study for 22 cytotoxic ruthenium complexes containing mono-, di- and tri-substituted hydroxyquinoline ligands demonstrated complexes that are highly potent. Nearly all of these complexes were found to possess activity at submicromolar concentrations, with IC_{50} values ranging from 58 to 96 nM in the HL60 cell line. Incorporation of a halogen at the 2-, 5-, or 7-position is associated with improvement of the activity, though the greatest impact was seen at the 2- and 7-positions (with 3–5-fold increases in potency). Placement of a methyl group at the 2-position resulted in a complex with the same potency as the unsubstituted HQ complex, suggesting that the halogen plays an electronic role rather than exerting some steric influence, as the van der Waals radius of $-CH_3$ (2.00 Å) is essentially the same as that of −Br (1.95 Å). However, addition of the large and asymmetric *o*-tolyl group at the 5- and 7- positions resulted in up to a 10-fold *loss* of activity. The 2-position appears to be the only site for incorporation of larger groups without loss of activity.

What is most striking from the SAR analysis is how distinct the activity profile is from both free HQ ligands and those contained in organometallic complexes (in contrast to the coordination complexes discussed here). Substituents at the 5-position are very commonly found in biologically active HQ free ligands, particularly those that act as neuroprotective or anticancer agents through metal coordination [27]; however, this study demonstrates that the biologically active HQ ligands with substituents at the 2-position, and none, to the best of our knowledge, that are Ru(II) coordination complexes. This provides a relatively unexplored region of chemical space to exploit.

Rational design of improved systems requires the identification of the biological target. Previously we explored and eliminated the possibility of DNA binding and proteasome inhibition, both of which had been hypothesized as mechanisms of action for other metal complexes containing HQ ligands or the free ligands themselves. Having excluded these as possible causes for cytotoxicity, we turned to a functional assay recently developed in our laboratory that monitors the production of a fluorescent protein, Dendra2. This is a global assay for transcription and translation, and reports on interference with any stage or biological component that plays a role in these processes. The most potent Ru(II) complexes were tested, and all were found to inhibit protein production (compounds **4**, **13**, **15**, **19**, and **20**; Fig. S6). The free HQ ligands that were incorporated into complexes **19** and **20** were also tested, and also inhibited protein production. It may be important that the ligands possessed cytotoxicity at 3–4-fold lower doses than demonstrated inhibition of translation, while the Ru(II) complexes were cytotoxic at 2–15-fold lower concentrations than those required to observe inhibition of Dendra2. The inhibition of protein synthesis may not be the exclusive cause for cytotoxicity of ruthenium complexes, and additional mechanisms might be involved for their antitumor activity. Alternatively, the discrepancy between the IC_{50} values may reflect the difference in the time frame for the two experiments (72 h for cytotoxicity, while changes in Dendra2 production were observed at time points less than 15 h). In either case, inhibition of translation is an appealing mechanism for anticancer agents, due in part to the fact that cancer cells have greater needs for ongoing protein synthesis for proliferation and cell survival that depend on specific regulatory proteins [28]. One translation inhibitor, omacetaxine mepesuccinate, is already in clinical use for chronic meyloid leukemia (CML) [29]. Very recently, cyclometalated Ru(II) complexes were reported that inhibit proteosynthesis [30]; this is a new mechanism of action for metal complexes, and the systems described in that report have similar cytotoxic potencies (albeit in other cell lines) to the compounds described here. While there many notable chemical differences, the overall charge on the molecules (+1) and general structures are alike, as both are octahedral complexes containing bidentate ligands. It is possible that both these classes of metal complexes are selectively inhibiting some components of the protein synthesis machinery. Studies are underway to further elucidate the target(s) of the HQ complexes.

4. Experimental section

4.1. Materials and methods

addition of oxygen rich substituents such as a nitro group or sulfonic acid is exceedingly detrimental to the activity of the HQ Ru(II) coordination complex. Arylation at this position was also disfavored, and the serendipitous synthesis of the 5-5-linked dimer **22** suggests that loss of activity may also scale with the size of the substituent, as the dimer was 15-fold less potent than the complex containing the *o*-tolyl group. These results combine to suggest that the coordination complex has a specific binding site on a particular biological target, and that introduction of steric clash or electron rich substituents on this face of the molecule disrupts key contacts.

There are also many reports of 7-substituted HQ systems with noteworthy biological activity, but in this study, the addition of groups larger than a halogen at this position reduced cytotoxicity for the Ru(II) complex. In contrast, the 2-position was found to be the best site for arylation, and thus, we hypothesize, addition of other substituents. There are comparatively few reports of

synthesized and described previously [1a].

All ^{1}H NMR spectra were obtained on a Varian Mercury spectrometer (400 MHz) with chemical shifts reported relative to the residual solvent peak of acetonitrile at δ 1.94. Electrospray ionization mass spectra were obtained on a Varian 1200 L mass spectrometer. Absorption spectra were obtained on an Agilent Cary 60 spectrophotometer. Extinction coefficients were determined from three independent replicates, and reported values are with 5% error. All synthesized compounds were isolated in >95% purity, as determined by analytical HPLC. For HPLC analysis, the ruthenium complexes were injected on an Agilent 1100 series HPLC equipped with a model G1311 quaternary pump, G1315B UV diode array detector, and ChemStation software version B.01.03. Chromatographic conditions were optimized on a Column Technologies Inc. C18, 120 Å (250 mm × 4.6 mm inner diameter, 5 μM) fitted with a Phenomenex C18 (4 mm × 3 mm) guard column. Injection volumes of 15 μL of 100 μM solutions of the complex were used. The detection wavelength was 280 nm. Mobile phases were: mobile phase A, 0.1% formic acid in dH_2O; mobile phase B, 0.1% formic acid in HPLC grade acetonitrile. The mobile phase flow rate was 1.0 mL/min. The following mobile phase gradient was used: 98–95% A (containing 2–5% B) from 0 to 5 min; 95–70% A (5–30% B) from 5 to 15 min; 70–40% A (30–60% B) from 15 to 20 min; 40–5% A (60–95% B) from 20 to 30 min; 5–98% A (95–2% B) from 30 to 35 min; reequilibration at 98% A (2% B) from 35 to 40 min.

4.2. General synthesis of [Ru(dmphen)$_2$L] complexes with HQ ligands

The synthesis of metal complexes was performed following a previously described procedure [1a]. **[**Ru(dmphen)$_2$Cl$_2$] (100 mg, 0.17 mmol) and HQ (0.19 mmol) were added to 4 mL of ethylene glycol in a 15 mL pressure tube. The mixture was heated at 100–120 °C for 2 h while protected from light. The purple solution was allowed to cool to room temperature and poured into 50 mL of dH_2O. Addition of a saturated aq. KPF_6 solution (ca. 1 mL) produced a purple precipitate that was collected by vacuum filtration. The purification of the solid was carried out by flash chromatography (silica gel, loaded in MeCN). A gradient was run, and the pure complex eluted at 0.2% KNO_3, 5–10% H_2O in MeCN. The product fractions were concentrated under reduced pressure, and a saturated aq. solution of KPF_6 was added, followed by extraction of the complex into CH_2Cl_2. The solvent was removed under reduced pressure to give the product as a solid.

The starting hydroxyquinoline ligands were obtained from commercial sources and were used without further purification. The ligands purchased were 5-bromo-8-hydroxyquinoline (Ark Pharm, 97%), 5-chloro-8-hydroxyquinoline (Aldrich, 95%), 7-bromo-8-hydroxyquinoline (Aldrich, 97%), 7-chloro-8-hydroxyquinoline (Toronto Research Chemicals), 5,7-dimethyl-8-hydroxyquinoline (Aldrich, 98%), 5,7-dibromo-8-hydroxyquinoline (MP Biomedicals), 5,7-dichloro-8-hydroxyquinoline (Acros Organics, 99%), 5,7-diiodo-8-hydroxyquinoline (Aldrich, 97%), 8-hydroxy-2,5,7-trimethylquinoline (Aurum Pharmatech), 5,7-dichloro-8-hydroxy-2-methylquinoline (Aldrich, 98%). The ligands 2-bromo-HQ [31], 2-chloro-HQ [32], 2-Cl-5,7-dibromo-HQ and 2-methyl-5,7-dibromo-HQ [33] were synthesized according to the described methods with minor modification. 2-o-Tolyl-HQ was synthesized using general Suzuki coupling procedure [34]. Complexes **1**, **2**, **14**, and **16** were

4.2.4. Compound 6

Yield: 81 mg (54%). ^{1}H NMR (CD_3CN): δ 8.44–8.48 (m, 2H), 8.31 (d, J = 8.3 Hz, 1H), 8.19 (d, J = 8.3 Hz, 1H), 8.15 (d, J = 8.7 Hz, 1H), 7.97–8.11 (m, 4H), 7.69 (d, J = 8.4 Hz, 1H), 7.60 (d, J = 8.2 Hz, 1H), 7.36 (d, J = 8.3 Hz, 2H), 7.31 (d, J = 8.6 Hz, 1H), 6.82 (dd, J = 8.4, 5.1 Hz, 1H), 6.70 (d, J = 5.0 Hz, 1H), 6.17 (d, J = 8.6 Hz, 1H), 2.70 (s, 3H), 2.19 (s, 3H), 1.96 (s, 3H), 1.82 (s, 3H); purity by HPLC = 98%; $C_{37}H_{29}BrN_5ORu$ $[M]^+$ 740.06, found 742.2 $[M]^+$; UV/Vis (CH_3CN): λ_{max} ($\varepsilon \times 10^{-3}$) 495 nm (10.6).

4.2.5. Compound 7

Yield: 87 mg (61%). ^{1}H NMR (CD_3CN): δ 8.43–8.47 (m, 2H), 8.30 (d, J = 8.3 Hz, 1H), 8.18 (d, J = 8.3 Hz, 1H), 8.14 (d, J = 8.8 Hz, 1H), 8.00–8.10 (m, 4H), 7.68 (d, J = 8.3 Hz, 1H), 7.60 (d, J = 8.3 Hz, 1H), 7.34–7.38 (m, 2H), 7.15 (d, J = 8.7 Hz, 1H), 6.82 (dd, J = 8.6, 5.1 Hz, 1H), 6.71 (dd, J = 5.1, 1.3 Hz, 1H), 6.18 (d, J = 8.6 Hz, 1H), 2.69 (s, 3H), 2.18 (s, 3H), 1.96 (s, 3H), 1.82 (s, 3H); purity by HPLC = 99%; ESI MS calcd for $C_{37}H_{29}ClN_5ORu$ $[M]^+$ 696.11, found 696.2 $[M]^+$; UV/Vis (CH_3CN): λ_{max} ($\varepsilon \times 10^{-3}$) 495 nm (11.3).

4.2.6. Compound 9

Yield: 78 mg (52%). ^{1}H NMR (CD_3CN): δ 8.45–8.48 (m, 2H), 8.29 (d, J = 8.2 Hz, 1H), 8.19 (d, J = 8.3 Hz, 1H), 8.15 (d, J = 8.7 Hz, 1H), 8.01–8.11 (m, 3H), 7.81 (d, J = 8.3 Hz, 1H), 7.68 (d, J = 8.3 Hz, 1H), 7.60 (d, J = 8.2 Hz, 1H), 7.29–7.37 (m, 3H), 7.15 (d, J = 8.7 Hz, 1H), 6.74 (dd, J = 8.3, 5.1 Hz, 1H), 6.68 (d, J = 4.9 Hz, 1H), 6.60 (d, J = 8.5 Hz, 1H), 2.65 (s, 3H), 2.19 (s, 3H), 1.92 (s, 3H), 1.83 (s, 3H); purity by HPLC = 97%; $C_{37}H_{29}BrN_5ORu$ $[M]^+$ 740.06, found 740.1 $[M]^+$; UV/Vis (CH_3CN): λ_{max} ($\varepsilon \times 10^{-3}$) 490 nm (12.8).

4.2.7. Compound 10

Yield: 69 mg (48%). ^{1}H NMR (CD_3CN): δ 8.44–8.48 (m, 2H), 8.29 (d, J = 8.3 Hz, 1H), 8.18 (d, J = 8.3 Hz, 1H), 8.14 (d, J = 8.7 Hz, 1H), 8.00–8.11 (m, 3H), 7.81 (dd, J = 8.3, 1.3 Hz, 1H), 7.68 (d, J = 8.3 Hz, 1H), 7.61 (d, J = 8.2 Hz, 1H), 7.32–7.36 (m, 2H), 7.19 (d, J = 8.5 Hz, 1H), 6.72 (dd, J = 8.2, 5.1 Hz, 1H), 6.67 (dd, J = 5.1, 1.3 Hz, 1H), 6.62

7.34 (d, $J = 8.3$ Hz, 1H), 6.86 (dd, $J = 8.6$, 5.1 Hz, 1H), 6.75 (dd, $J = 5.1$, 1.2 Hz, 1H), 2.62 (s, 3H), 2.19 (s, 3H), 1.96 (s, 3H), 1.82 (s, 3H); purity by HPLC = 97%; ESI MS calcd for $C_{37}H_{28}Br_2N_5ORu$ $[M]^+$ 817.97, found 820.0 $[M]^+$; UV/Vis (CH_3CN): λ_{max} ($\varepsilon \times 10^{-3}$) 490 nm (14.0).

4.2.10. Compound 15

Yield: 63 mg (40%). ^{1}H NMR (CD_3CN): δ 8.47 (d, $J = 8.3$ Hz, 2H), 8.30 (d, $J = 8.3$ Hz, 1H), 8.20 (d, $J = 8.3$ Hz, 1H), 8.15 (d, $J = 8.8$ Hz, 1H), 8.02–8.11 (m, 4H), 7.69 (d, $J = 8.3$ Hz, 1H), 7.61 (d, $J = 8.3$ Hz, 1H), 7.45 (s, 1H), 7.36 (d, $J = 8.3$ Hz, 1H), 7.34 (d, $J = 8.3$ Hz, 1H), 6.86 (dd, $J = 8.6$, 5.1 Hz, 1H), 6.77 (dd, $J = 5.1$, 1.2 Hz, 1H), 2.62 (s, 3H), 2.19 (s, 3H), 1.92 (s, 3H), 1.82 (s, 3H); purity by HPLC = 97%; ESI MS calcd for $C_{37}H_{28}BrClN_5ORu$ $[M]^+$ 774.02, found 776.1 $[M]^+$; UV/Vis (CH_3CN): λ_{max} ($\varepsilon \times 10^{-3}$) 490 nm (12.9).

4.2.11. Compound 17

Yield: 68 mg (38%). ^{1}H NMR (CD_3CN): δ 8.48 (d, $J = 8.3$ Hz, 2H), 8.28 (d, $J = 8.3$ Hz, 1H), 8.20 (d, $J = 8.3$ Hz, 1H), 8.16 (d, $J = 8.8$ Hz, 1H), 8.10 (d, $J = 8.8$ Hz, 1H), 8.02–8.05 (m, 2H), 7.90 (s, 1H), 7.85 (dd, $J = 8.6$, 1.1 Hz, 1H), 7.70 (d, $J = 8.3$ Hz, 1H), 7.60 (d, $J = 8.3$ Hz, 1H), 7.35 (d, $J = 8.3$ Hz, 1H), 7.30 (d, $J = 8.3$ Hz, 1H), 6.84 (dd, $J = 8.6$, 5.1 Hz, 1H), 6.70 (dd, $J = 5.1$, 1.1 Hz, 1H), 2.57 (s, 3H), 2.23 (s, 3H), 1.88 (s, 3H), 1.81 (s, 3H); purity by HPLC = 98%; ESI MS calcd for $C_{37}H_{28}I_2N_5ORu$ $[M]^+$ 913.94, found 914.0 $[M]^+$; UV/Vis (CH_3CN): λ_{max} ($\varepsilon \times 10^{-3}$) 490 nm (15.2).

4.2.12. Compound 18

Yield: 74 mg (51%). ^{1}H NMR (CD_3CN): δ 8.36–8.40 (m, 2H), 8.26 (d, $J = 8.3$ Hz, 1H), 8.22 (d, $J = 8.3$ Hz, 1H), 7.97–8.11 (m, 4H), 7.87 (d, $J = 8.7$ Hz, 1H), 7.39–7.43 (m, 2H), 7.27 (d, $J = 8.2$ Hz, 1H), 6.81 (s, 1H), 6.85 (d, $J = 8.7$ Hz, 1H), 2.65 (s, 3H), 2.32 (s, 3H), 2.28 (s, 3H), 2.17 (s, 3H), 1.50 (s, 3H), 1.46 (s, 3H), 1.18 (s, 3H); purity by HPLC = 99%; ESI MS calcd for $C_{40}H_{36}N_5ORu$ $[M]^+$ 704.2, found 704.3 $[M]^+$; UV/Vis (CH_3CN): λ_{max} ($\varepsilon \times 10^{-3}$) 505 nm (11.0).

4.2.13. Compound 19

Yield: 70 mg (42%). ^{1}H NMR (CD_3CN): δ 8.40–8.42 (m, 2H), 8.27–8.30 (m, 2H), 8.00–8.12 (m, 5H), 7.70 (d, $J = 8.3$ Hz, 1H), 7.52 (s, 1H), 7.42–7.45 (m, 2H), 7.35 (d, $J = 8.3$ Hz, 1H), 7.85 (d, $J = 8.8$ Hz, 1H), 2.60 (s, 3H), 2.28 (s, 3H), 2.20 (s, 3H), 1.50 (s, 3H), 1.25 (s, 3H); purity by HPLC = 96%; ESI MS calcd for $C_{38}H_{30}Br_2N_5ORu$ $[M]^+$ 831.99, found 834.0 $[M]^+$; UV/Vis (CH_3CN): λ_{max} ($\varepsilon \times 10^{-3}$) 490 nm (13.6).

4.2.8. Compound 12

Yield: 60 mg (42%). ^{1}H NMR (CD_3CN): δ 8.44 (d, $J = 8.2$ Hz, 2H), 8.24 (d, $J = 8.3$ Hz, 1H), 8.17 (d, $J = 8.3$ Hz, 1H), 8.14 (d, $J = 8.8$ Hz, 1H), 8.09 (d, $J = 8.7$ Hz, 1H), 8.00–8.02 (m, 2H), 7.86 (dd, $J = 8.5$, 1.2 Hz, 1H), 7.68 (d, $J = 8.3$ Hz, 1H), 7.58 (d, $J = 8.3$ Hz, 1H), 7.33 (d, $J = 8.3$ Hz, 1H), 7.26 (d, $J = 8.3$ Hz, 1H), 6.89 (s, 1H), 6.65 (dd, $J = 8.5$, 5.1 Hz, 1H), 6.60 (dd, $J = 5.1$, 1.2 Hz, 1H), 2.67 (s, 3H), 2.32 (s, 3H), 2.21 (s, 3H), 1.88 (s, 3H), 1.83 (s, 3H), 1.61 (s, 3H); purity by HPLC = 97%; ESI MS calcd for $C_{39}H_{34}N_5ORu$ $[M]^+$ 690.18, found 690.2 $[M]^+$; UV/Vis (CH_3CN): λ_{max} ($\varepsilon \times 10^{-3}$) 500 nm (9.0).

4.2.9. Compound 13

Yield: 93 mg (57%). ^{1}H NMR (CD_3CN): δ 8.46–8.49 (m, 2H), 8.31 (d, $J = 8.3$ Hz, 1H), 8.21 (d, $J = 8.3$ Hz, 1H), 8.16 (d, $J = 8.8$ Hz, 1H), 8.11 (d, $J = 8.8$ Hz, 1H), 8.02–8.06 (m, 2H), 7.99 (dd, $J = 8.6$, 1.2 Hz, 1H), 7.69 (d, $J = 8.3$ Hz, 1H), 7.60–7.62 (m, 2H), 7.37 (d, $J = 8.3$ Hz, 1H), (d, $J = 7.9$ Hz, 1H), 2.67 (s, 3H), 2.52 (s, 3H), 2.18 (s, 3H), 1.83 (s, 3H); purity by HPLC = 97%; ESI MS calcd for $C_{37}H_{29}ClN_5ORu$ $[M]^+$ 696.11, found 696.1 $[M]^+$; UV/Vis (CH_3CN): λ_{max} ($\varepsilon \times 10^{-3}$) 495 nm (13.6).

(1:1) in a 15 mL pressure tube. The mixture was heated at 60 °C for 5 h while protected from light. The purple solution was allowed to cool to room temperature and poured into 50 mL of dH_2O. Addition of a saturated aq. KPF_6 solution (ca. 1 mL) produced a purple precipitate that was collected by vacuum filtration. The purification of the solid was carried out by flash chromatography (silica gel, loaded in MeCN). A gradient was run, and the pure complex eluted at 0.2% KNO_3, 8–10% H_2O in MeCN. The product fractions were concentrated under reduced pressure, and a saturated aq. solution of KPF_6 was added, followed by extraction of the complex into CH_2Cl_2. The solvent was removed under reduced pressure to give a purple solid. Yield: 64 mg (45%). ^{1}H NMR (CD_3CN): δ 8.43–8.48 (m, 2H), 8.30–8.32 (m, 1H), 7.98–8.19 (m, 5H), 7.67 (dd, $J = 8.3$, 2.5 Hz, 1H), 7.61 (d, $J = 8.9$ Hz, 1H), 7.34–7.39 (m, 2H), 6.96–7.25 (m, 2H), 6.63–6.68 (m, 1H), 6.48–6.59 (m, 1H), 2.69–2.70 (m, 3H), 2.16 (s, 3H), 1.93 (s, 3H), 1.82 (s, 3H); purity by HPLC = 96%; ESI MS calcd for $C_{74}H_{56}Cl_2N_{10}O_2Ru_2$ $[M]^{2+}$ 695.11, found 695.1 $[M]^{2+}$; UV/Vis (CH_3CN): λ_{max} ($\varepsilon \times 10^{-3}$) 495 nm (12).

4.3. Compounds 8 and 11

The synthesis was performed using general Suzuki coupling procedure [34]. Complex **6** or **9** (34 μmol), o-tolylboronic acid (70 mg, 51 μmol), $[Pd(PPh_3)_4]$ (3.4 mg, 0.34 μmol) and K_2CO_3 (14 mg, 102 μmol) were added to a flask under argon. Methanol (3 mL; degassed) was added to the reaction mixture via cannula. The resulting mixture was refluxed with stirring for 48 h, followed by removal of the solvent under reduced pressure to give a purple solid. Purification was carried out by flash chromatography (silica gel, loaded in MeCN, followed by a gradient); the pure complex eluted at 0.2% KNO_3, 1% H_2O in MeCN. The product fractions were combined and concentrated under reduced pressure. A saturated aq. solution of KPF_6 was added, and the complex was extracted into CH_2Cl_2, followed by removal of the solvent under reduced pressure to give a purple solid.

4.3.1. Compound 8

Yield: 16 mg (53%). ^{1}H NMR (CD_3CN): ^{1}H NMR (CD_3CN): δ 8.39–8.46 (m, 2H), 8.29 (d, $J = 8.3$ Hz, 1H), 7.99–8.21 (m, 5H), 7.70 (d, $J = 8.2$ Hz, 1H), 7.58 (d, $J = 8.3$ Hz, 1H), 7.35–7.42 (m, 2H), 7.17–7.29 (m, 5H), 6.96–7.05 (m, 2H), 6.59–6.66 (m, 1H), 6.54 (brs,

(11.2).

4.2.14. Compound 20

Yield: 70 mg (46%). ^{1}H NMR (CD_3CN): δ 8.42 (d, $J = 8.3$ Hz, 2H), 8.31 (d, $J = 8.3$ Hz, 1H), 8.28 (d, $J = 8.3$ Hz, 1H), 8.02–8.12 (m, 5H), 7.70 (d, $J = 8.3$ Hz, 1H), 7.42–7.47 (m, 2H), 7.38 (d, $J = 8.3$ Hz, 1H), 7.28 (s, 1H), 7.84 (d, $J = 8.8$ Hz, 1H), 2.64 (s, 3H), 2.26 (s, 3H), 2.23 (s, 3H), 1.52 (s, 3H), 1.24 (s, 3H); purity by HPLC = 99%; ESI MS calcd for $C_{38}H_{30}Cl_2N_5ORu$ $[M]^+$ 744.09, found 744.2 $[M]^+$; UV/Vis (CH_3CN): λ_{max} ($\varepsilon \times 10^{-3}$) 490 nm (12.2).

4.2.15. Compound 21

Yield: 81 mg (48%). ^{1}H NMR (CD_3CN): δ 8.42 (d, $J = 8.3$ Hz, 1H), 8.40 (d, $J = 8.3$ Hz, 1H), 8.30–8.34 (m, 2H), 8.02–8.11 (m, 5H), 7.67 (d, $J = 8.3$ Hz, 1H), 7.61 (s, 1H), 7.45–7.48 (m, 2H), 7.40 (d, $J = 8.3$ Hz, 1H), 6.94 (d, $J = 9.0$ Hz, 1H), 2.62 (s, 3H), 2.39 (s, 3H), 2.27 (s, 3H), 1.55 (s, 3H); purity by HPLC = 99%; ESI MS calcd for $C_{37}H_{27}Br_2ClN_5ORu$ $[M]^+$ 851.93, found 854.0 $[M]^+$; UV/Vis (CH_3CN): λ_{max} ($\varepsilon \times 10^{-3}$) 470 nm (12.5).

4.2.16. Compound 22

$[Ru(dmphen)_2Cl_2]$ (100 mg, 0.17 mmol) and 7-chloro-HQ (30.5 mg, 0.17 mmol) were added to 8 mL of ethanol-water mixture

1H), 2.80 (s, 3H), 2.23 (s, 3H), 2.05 (s, 1.2H), 1.98 (s, 1.8H), 1.89 (s, 1.8H), 1.82 (s, 3 H), 1.78 (s, 1.2 H); purity by HPLC = 97%; ESI MS calcd for $C_{44}H_{36}N_5ORu$ $[M]^+$ 752.2, found 752.3 $[M]^+$; UV/Vis (CH_3CN): λ_{max} ($\varepsilon \times 10^{-3}$) 495 nm (7.6).

4.3.2. Compound 11

Yield: 13 mg (43%). ^{1}H NMR (CD_3CN): δ 8.44 (d, $J = 8.2$ Hz, 1H), 8.33–8.37 (m, 2H), 8.10–8.18 (m, 2H), 8.04 (d, $J = 8.8$ Hz, 1H), 8.01 (d, $J = 8.8$ Hz, 1H), 7.80 (d, $J = 8.3$ Hz, 1H), 7.68 (d, $J = 8.3$ Hz, 1H), 7.48 (d, $J = 8.3$ Hz, 1H), 7.40 (d, $J = 8.2$ Hz, 1H), 7.32 (d, $J = 8.3$ Hz, 1H), 6.82–7.02 (m, 5H), 6.65–6.73 (m, 3H), 6.28 (brs, 1H), 2.48 (s, 3H), 2.15 (s, 6H), 2.02 (s, 3H), 1.75 (s, 3H); purity by HPLC = 98%; ESI MS calcd for $C_{44}H_{36}N_5ORu$ $[M]^+$ 752.2, found 752.3 $[M]^+$; UV/Vis (CH_3CN): λ_{max} ($\varepsilon \times 10^{-3}$) 490 nm (6.8).

4.4. Counter ion exchange

Compounds **1**–**22** were converted to Cl^- salts by dissolving 5–10 mg of product in 1–2 mL methanol. The dissolved product was loaded onto an Amberlite IRA-410 chloride ion exchange column, eluted with methanol, and the solvent removed under reduced pressure.

4.5. Cytotoxicity assay

HL60 cells were plated at 30,000 cell per well in optiMEM (supplemented with 2% FBS, 50 U/ml Penicillin and 50 mg/ml Streptomycin) in 96 well plates. Compounds were serially diluted in optiMEM in a 96 well plate and then added to the cells. The cells were incubated with the compounds for 72 h followed by the addition of resazurin. The plates were incubated for 3 h and then read on a SpectraFluor Plus plate reader with an excitation filter of 535 nm and emission of 595 nm.

4.6. Dendra 2 transcription-translation assay

96 well plates were coated with matrigel followed by the addition of HEK T-Rex cells at a density of 30,000 cells/well and incubated with 1 μg/mL of tetracycline for 16 h. Media was removed and 50 μL of L-15 media containing 1 μg/mL tetracycline along with compound was added to each well and allowed to incubate for 1 h. Plates were then illuminated with a 405 nm LED flood array for one 1 min and then read in kinetic mode on a SpectraFluor Plus (Tecan) set to 37 C. The plates were read every 30 min for 15 h with excitation and emission wavelengths of 480 nm and 530 nm for newly translated Dendra2 and 535 nm and 595 nm for post-translated Dendra2.

4.7. Crystallography

Single crystals of compounds **2**, **9** and **14** were grown from methylene chloride or acetone by vapor diffusion of diethyl ether. They were mounted in inert oil and transferred to the cold gas stream of the diffractometer. X-ray diffraction data were collected at 90.0(2) K on either a Nonius kappaCCD diffractometer using Mo$K\alpha$ X-rays or on a Bruker-Nonius X8 Proteum diffractometer with graded-multilayer focused Cu$K\alpha$ X-rays. Raw data were integrated, scaled, merged and corrected for Lorentz-polarization effects using either the HKL-SMN package [35] or the APEX2 package [36]. Corrections for absorption were applied using SADABS [37] and XABS2 [38]. The structures were solved by SHELXT [39], and refined against F^2 by weighted full-matrix least-squares using

[I > 2 σ(I)], $R_1 = 0.0337$ and $wR_2 = 0.0891$ (all indices), largest difference peak/hole = 0.689/-0.611 eÅ^{-3}.

4.7.3. Crystal data (14)

$C_{43}H_{41}Cl_2F_6N_5O_2PRu$, Mr = 976.75, Monoclinic, I2/a, a = 23.4088(6) Å, b = 10.0546(2) Å, c = 34.4516(12) Å, α = 90°, β = 90.859(1)°, γ = 90°, V = 8107.8(4) Å^3, Z = 8, ρ = 1.60 mg m^{-3}, μ = 5.349 mm^{-1}, F(000) = 3976, crystal size = 0.090 × 0.080 × 0.045 mm, θ(max) = 68.321°, 54029 reflections collected, 7380 unique reflections ($R_{int} = 0.0379$), GOF = 1.028, $R_1 = 0.0262$ and $wR_2 = 0.0706$ [I > 2 σ(I)], $R_1 = 0.0269$ and $wR_2 = 0.0711$ (all indices), largest difference peak/hole = 0.544/-0.518 eÅ^{-3}.

Acknowledgment

This work was supported by the American Cancer Society (RSG-13-079-01-CDD). Mass spectrometry analysis was performed at the University of Kentucky Environmental Research Training Laboratory (ERTL).

Abbreviations

HQ	8-hydroxyquinoline
SAR	structure-activity relationships
bpy	2,2′- bipyridine
phen	1,10-phenanthroline
dmphen	2,9-dimethyl-1,10-phenanthroline
IC_{50}	inhibitory concentration for 50% reduction

Appendix A. Supplementary data

Supplementary data related to this article can be found at https://doi.org/10.1016/j.ejmech.2018.04.044.

References

[1] a) D.K. Heidary, B.S. Howerton, E.C. Glazer, J. Med. Chem. 57 (2014) 8936–8946;
b) O. Afzal, S. Kumar, M.R. Haider, M.R. Ali, R. Kumar, M. Jaggi, S. Bawa, Eur. J. Med. Chem. 97 (2015) 871–910.

SHELXL-2014 [40]. For compound **8** the SQUEEZE routine [41] was used to treat disordered solvent. Hydrogen atoms were placed at calculated positions and refined using a riding model. Non-hydrogen atoms were refined with anisotropic displacement parameters. Structures were checked using check CIF tools in Platon [42] and by an R-tensor [43]. Crystal data and relevant details of the structure determinations are summarized below and selected geometrical parameters are given in Table 1.

4.7.1. Crystal data (2)

$C_{39}H_{34}Cl_2F_6N_5OPRu$, Mr = 905.65, Monoclinic, P21/c, a = 16.2343(3) Å, b = 13.0460(3) Å, c = 17.6161(3) Å, α = 90°, β = 105.283(1)°, γ = 90°, V = 4180.29(12) Å^3, Z = 4, ρ = 1.671 mg m^{-3}, μ = 5.951 mm^{-1}, F(000) = 1832, crystal size = 0.100 × 0.080 × 0.020 mm, θ(max) = 68.210°, 46939 reflections collected, 6555 unique reflections (R_{int} = 0.0397), GOF = 1.079, R_1 = 0.0302 and wR_2 = 0.081 [I > 2σ(I)], R_1 = 0.0316 and wR_2 = 0.0826 (all indices), largest difference peak/hole = 0.726/-0.681 eÅ^{-3}.

4.7.2. Crystal data (9)

$C_{38}H_{31}BrCl_2F_6N_5OPRu$, Mr = 970.53, Monoclinic, P2(1)/n, a = 15.1996(4) Å, b = 12.8658(3) Å, c = 19.7650(5) Å, α = 90°, β = 109.65(1)°, γ = 90°, V = 3640.05(16) Å^3, Z = 4, ρ = 1.771 mg m^{-3}, μ = 7.171 mm^{-1}, F(000) = 1936, crystal size = 0.290 × 0.180 × 0.070 mm, θ(max) = 68.231°, 47643 reflections collected, 6626 unique reflections (R_{int} = 0.0506), GOF = 1.087, R_1 = 0.0322 and wR_2 = 0.0879

[2] A.R. Timerbaev, Metallomics 1 (2009) 193–198.
[3] H. Sheshbaradaran, R. Baerga, J. Cobb, in: Method for Treating Pancreatic Cancer Using a Gallium Complex, Niiki Pharma Inc., USA, 2011, p. 16.
[4] a) B. Kubista, T. Schoefl, L. Mayr, S. van Schoonhoven, P. Heffeter, R. Windhager, B.K. Keppler, W. Berger, J. Exp. Clin. Canc. Res. 36 (2017) 52;
b) N. Wilfinger, S. Austin, B. Scheiber-Mojdehkar, W. Berger, S. Reipert, M. Praschberger, J. Paur, R. Trondl, B.K. Keppler, C.C. Zielinski, K. Nowikovsky, Oncotarget 7 (2016) 1242–1261.
[5] Y.-L. Li, Q.-P. Qin, Y.-F. An, Y.-C. Liu, G.-B. Huang, X.-J. Luo, G.-H. Zhang, Inorg. Chem. Commun. 40 (2014) 73–77.
[6] S. Tardito, A. Barilli, I. Bassanetti, M. Tegoni, O. Bussolati, R. Franchi-Gazzola, C. Mucchino, L. Marchiò, J. Med. Chem. 55 (2012) 10448–10459.
[7] a) Q.-P. Qin, Z.-F. Chen, J.-L. Qin, X.-J. He, Y.-L. Li, Y.-C. Liu, K.-B. Huang, H. Liang, Eur. J. Med. Chem. 92 (2015) 302–313;
b) C.M. Santos, S. Cabrera, C. Rios-Luci, J.M. Padron, I.L. Solera, A.G. Quiroga, M.A. Medrano, C. Navarro-Ranninger, J. Aleman, Dalton trans. 42 (2003) 13343–13348;
c) T. Meng, S.-F. Tang, Q.-P. Qin, Y.-L. Liang, C.-X. Wu, C.-Y. Wang, H.-T. Yan, J.-X. Dong, Y.-C. Liu, MedChemComm 7 (2016) 1802–1811.
[8] a) H.-R. Zhang, T. Meng, Y.-C. Liu, Z.-F. Chen, Y.-N. Liu, H. Liang, Appl. Organomet. Chem. 30 (2016) 740–747;
b) H.-R. Zhang, K.-B. Huang, Z.-F. Chen, Y.-C. Liu, Y.-N. Liu, T. Meng, Q.-P. Qin, B.-Q. Zou, H. Liang, MedChemComm 7 (2016) 806–812.
[9] H.-R. Zhang, Y.-C. Liu, T. Meng, Q.-P. Qin, S.-F. Tang, Z.-F. Chen, B.-Q. Zou, Y.-N. Liu, H. Liang, MedChemComm 6 (2015) 2224–2231.
[10] C. Martin-Santos, E. Michelucci, T. Marzo, L. Messori, P. Szumlas, P.J. Bednarski, R. Mas-Balleste, C. Navarro-Ranninger, S. Cabrera, J. Aleman, J. Inorg. Biochem. 153 (2015) 339–345.
[11] a) H.-R. Zhang, Y.-C. Liu, Z.-F. Chen, T. Meng, B.-Q. Zou, Y.-N. Liu, H. Liang, N. J. Chem. 40 (2016) 6005–6014;
b) Y.-L. Zhang, Q.-P. Qin, Q.-q. Cao, H.-H. Han, Z.-L. Liu, Y.-C. Liu, H. Liang, Z.-F. Chen, MedChemComm 8 (2017) 184–190.
[12] a) Z.-F. Chen, X.-Y. Song, Y. Peng, X. Hong, Y.-C. Liu, H. Liang, Dalton Trans. 40 (2011) 1684–1692;
b) Z.-F. Chen, Y.-Q. Gu, X.-Y. Song, Y.-C. Liu, Y. Peng, H. Liang, Eur. J. Med. Chem. 59 (2013) 194–202;
c) Z.-F. Chen, Y. Peng, Y.-Q. Gu, Y.-C. Liu, M. Liu, K.-B. Huang, K. Hu, H. Liang, Eur. J. Med. Chem. 62 (2013) 51–58.
[13] Y.-C. Liu, Z.-F. Chen, X.-Y. Song, Y. Peng, Q.-P. Qin, H. Liang, Eur. J. Med. Chem. 59 (2013) 168–175.
[14] Y.-C. Liu, X.-Y. Song, Z.-F. Chen, Y.-Q. Gu, Y. Peng, H. Liang, Inorg. Chim. Acta. 382 (2012) 52–58.
[15] Y.-C. Liu, J.-H. Wei, Z.-F. Chen, M. Liu, Y.-Q. Gu, K.-B. Huang, Z.-Q. Li, H. Liang, Eur. J. Med. Chem. 69 (2013) 554–563.
[16] Z.-F. Chen, J.-H. Wei, Y.-C. Liu, M. Liu, Y.-Q. Gu, K.-B. Huang, M. Wang, H. Liang, Eur. J. Med. Chem. 68 (2013) 454–462.
[17] B.-Q. Zou, Q.-P. Qin, Y.-X. Bai, Q.-Q. Cao, Y. Zhang, Y.-C. Liu, Z.-F. Chen, H. Liang, MedChemComm 8 (2017) 633–639.
[18] M. Kubanik, H. Holtkamp, T. Söhnel, S.M.F. Jamieson, C.G. Hartinger, Organometallics 34 (2015) 5658–5668.
[19] a) M. Gobec, J. Kljun, I. Sosic, I. Mlinaric-Rascan, M. Ursic, S. Gobec, I. Turel, Dalton Trans. 43 (2014) 9045–9051;
b) O. Domotor, V.F.S. Pape, N.V. May, G. Szakacs, E.A. Enyedy, Dalton Trans. 46 (2017) 4382–4396.
[20] L. Yang, J. Zhang, C. Wang, X. Qin, Q. Yu, Y. Zhou, J. Liu, Metallomics 6 (2014) 518–531.
[21] A.N. Hidayatullah, E. Wachter, D.K. Heidary, S. Parkin, E.C. Glazer, Inorg. Chem. 53 (2014) 10030–10032.
[22] D. Havrylyuk, D.K. Heidary, L. Nease, S. Parkin, E.C. Glazer, Eur. J. Inorg. Chem. 2017 (2017) 1687–1694.
[23] R.S. Talekar, G.S. Chen, S.Y. Lai, J.W. Chern, J. Org. Chem. 70 (2005) 8590–8593.
[24] a) S. Zhai, L. Yang, Q.C. Cui, Y. Sun, Q.P. Dou, B. Yan, J. Biol. Inorg. Chem. 15 (2010) 259–269;
b) X. Mao, X. Li, R. Sprangers, X. Wang, A. Venugopal, T. Wood, Y. Zhang, D.A. Kuntz, E. Coe, S. Trudel, D. Rose, R.A. Batey, L.E. Kay, A.D. Schimmer, Leukemia 23 (2009) 585–590;
c) K.G. Daniel, D. Chen, S. Orlu, Q.C. Cui, F.R. Miller, Q.P. Dou, Breast Cancer Res. 7 (2005) R897–R908.
[25] B. Cao, J. Li, X. Zhou, J. Juan, K. Han, Z. Zhang, Y. Kong, J. Wang, X. Mao, Sci. Rep. 4 (2014) 5749.
[26] D.K. Heidary, A. Fox, C.I. Richards, E.C. Glazer, SLAS Discov. 22 (2017) 399–407.
[27] V. Prachayasittikul, S. Prachayasittikul, S. Ruchirawat, V. Prachayasittikul, Drug Des. Dev. Ther. 7 (2013) 1157–1178.
[28] M. Bhat, N. Robichaud, L. Hulea, N. Sonenberg, J. Pelletier, I. Topisirovic, Nat. Rev. Drug Discov. 14 (2015) 261–278.
[29] V. Gandhi, W. Plunkett, J.E. Cortes, Clin. Canc. Res. 20 (2014) 1735–1740.
[30] V. Novohradsky, J. Yellol, O. Stuchlikova, M.D. Santana, H. Kostrhunova, G. Yellol, J. Kasparkova, D. Bautista, J. Ruiz, V. Brabec, Chemistry 23 (2017) 15294–15299.
[31] G. Verniest, X. Wang, N. De Kimpe, A. Padwa, J. Org. Chem. 75 (2010) 424–433.
[32] Y. Kudo, S. Furumoto, N. Okamura, Preparation of Fluorine-containing Quinoline Derivatives as Tau Imaging Probes for Positron-emission Tomography (PET), 2012.
[33] N.M. Shavaleev, R. Scopelliti, F. Gumy, J.C. Bunzli, Inorg. Chem. 48 (2009) 2908–2918.
[34] A. Suzuki, Acc. Chem. Res. 15 (1982) 178–184.
[35] Z.O.W. Minor, in: J.R.M.S.C.W. Carter (Ed.), Processing of X-ray Diffraction Data Collected in Oscillation Mode, vol. 276, Academic Press, 1997.
[36] APEX2, Programs for Data Collection and Data Reduction, Bruker-Nonius, Madison WI, USA, 2012.
[37] L. Krause, R. Herbst-Irmer, G.M. Sheldrick, D. Stalke, J. Appl. Cryst. 48 (2015) 3–10.
[38] S. Parkin, B. Moezzi, H. Hope, J. Appl. Cryst. 28 (1995) 53–56.
[39] G.M. Sheldrick, Acta Cryst. A71 (2015) 3–8.
[40] G.M. Sheldrick, Acta Cryst. C71 (2015).
[41] P. van der Sluis, A.L. Spek, Acta Cryst. A46 (1990) 194–201.
[42] A.L. Spek, Acta Cyst. D65 (2009) 148–155.
[43] S. Parkin, Acta Cyst. A56 (2000) 157–162.